Phase transition in traffic jam experiment on a circuit

Shin-ichi Tadaki[1,9]**, Macoto Kikuchi**[2]**, Minoru Fukui**[3]**,
Akihiro Nakayama**[4]**, Katsuhiro Nishinari**[5]**, Akihiro Shibata**[6]**,
Yuki Sugiyama**[7]**, Taturu Yosida**[3] **and Satoshi Yukawa**[8]

[1] Computer and Network Center, Saga University, Saga 840-8502, Japan
[2] Cybermedia Center, Osaka University, Toyonaka 560-0043, Japan
[3] Nakanihon Automotive College, Sakahogi 505-0077, Japan
[4] Faculty of Science and Technology, Meijo University, Nagoya 468-8502, Japan
[5] Research Center for Advanced Science and Technology, The University of Tokyo, Meguro 153-8904, Japan
[6] Computer Research Center, High Energy Accelerator Research Organization, KEK, Ibaraki 305-0801 Japan
[7] Department of Complex Systems Science, Nagoya University, Nagoya 464-8601, Japan
[8] Department of Earth and Space Science, Osaka University, Toyonaka 560-0043, Japan
E-mail: tadaki@cc.saga-u.ac.jp

Abstract. The emergence of a traffic jam is considered to be a dynamical phase transition in a physics point of view; traffic flow becomes unstable and changes phase into a traffic jam when the car density exceeds a critical value. In order to verify this view, we have been performing a series of circuit experiments. In our previous work (2008 *New J. Phys.* **10** 033001), we demonstrated that a traffic jam emerges even in the absence of bottlenecks at a certain high density. In this study, we performed a larger indoor circuit experiment in the Nagoya Dome in which the positions of cars were observed using a high-resolution laser scanner. Over a series of sessions at various values of density, we found

[9] Author to whom any correspondence should be addressed.

IOP Institute of Physics Φ DEUTSCHE PHYSIKALISCHE GESELLSCHAFT

that jammed flow occurred at high densities, whereas free flow was conserved at low densities. We also found indications of metastability at an intermediate density. The critical density is estimated by analyzing the fluctuations in speed and the density–flow relation. The value of this critical density is consistent with that observed on real expressways. This experiment provides strong support for physical interpretations of the emergence of traffic jams as a dynamical phase transition.

Contents

1. Introduction

A traffic jam is one of the most familiar phenomena observed on expressways and in city streets. Traffic flow can be divided into two types: smooth flow, which occurs under light traffic and in which cars run at the allowed maximum speed; and jammed flow, which occurs under heavy traffic conditions. In jammed flow, jam clusters in which cars stop or move slowly propagate in the direction opposite to that of the motion of the cars.

Fundamental diagrams describing the density–flow relation are widely used for analyzing traffic flow [1]. Observations of real expressway traffic show that fundamental diagrams (e.g. figure 1) have two regions mutually divided by a certain density value: free (smooth) flow with low density, and jammed flow with high density. In low density traffic, cars run at an almost constant speed, and therefore the flow increases in proportion to the density. The flow for high density traffic, on the other hand, decreases with the density, causing the average speed to also decrease with the density. The data points from high density traffic are broadly scattered; i.e. the speed and density fluctuate widely in jammed flow owing to the existence of jam clusters.

Since the 1990s many researchers have studied traffic flow from a physics point of view [2–8] and various theoretical models for traffic flow have been proposed and studied. This research has clarified that a homogeneous flow becomes unstable, leading to a traffic jam, if the density exceeds a critical value; as such, the emergence of traffic jams is understood as a dynamical phase transition in which density is the control parameter.
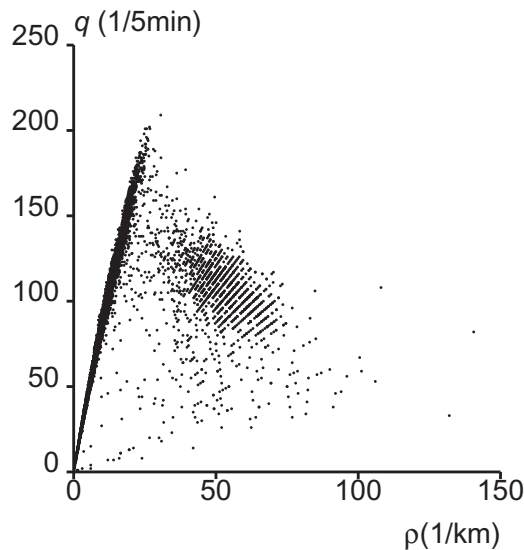
Figure 1. Typical fundamental diagram representing the relation between flow and car density based on 1 month of data measured in August (1996) at the 172.65 km post on the Tomei expressway. The critical density is nearly 25 cars km^{-1}. The data were provided by the Japan Highway Public Cooperation.

In a previous study we performed a traffic jam experiment using real cars on a 230 m circumference outdoor circuit [9, 10] in order to verify the theoretical understanding of traffic jams as a dynamical phase transition. In the study, we confirmed that traffic jams emerge at a certain high density even in the absence of bottlenecks, and we observed the metastable homogeneous flow that appears as a precursor to traffic jams. In order to confirm that the emergence of traffic jams is a dynamical phase transition, an experimental investigation of the density dependence of flow is required. To this end, we performed an extended experiment with a varying number of cars within an improved experimental environment: a circuit in the Nagoya Dome[10], an indoor Japanese Professional League baseball field. The new circuit was larger (314 m in circumference) than that used in the previous experiment, and we used a laser scanner to obtain higher-resolution positioning of the cars. Based on the experimental data recorded using this new setup, we can estimate the critical density of the phase transition between free and jammed flows.

This paper is organized as follows. In section 2, the details of the experiment are described. The data are analyzed in order to estimate the critical density in section 3. Finally, section 4 provides a summary and discussions.

2. The experiment

In order to study the effects of density on traffic flow, circuit inhomogeneity should be reduced as much as possible, as it may lead to bottlenecking; we therefore needed to use a circular road on flat ground with homogeneous lanes. In order to access the flat, concrete floor of the Nagoya Dome (see footnote 10), the pitching mound and artificial turf were removed and

[10] Nagoya Dome Ltd (www.nagoya-dome.co.jp/).
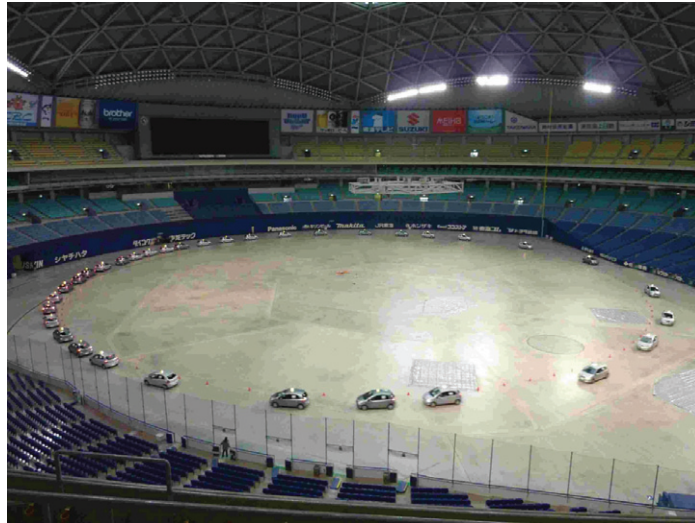
Figure 2. Bird's-eye view of 50 m radius (314 m circumference) circuit in the Nagoya Dome. The field is flattened by removing the pitching mound and artificial turf.
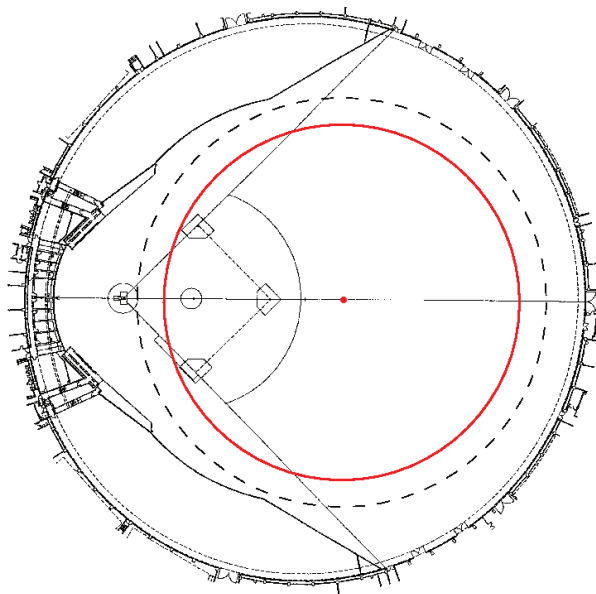
Figure 3. Plan of 50 m radius circuit (red curve) in the Nagoya Dome arena. The broken curve denotes a circle with a 60 m radius that delineates the outer range of the course. The laser scanner is located at the center of the circuit and is marked by a red point.

the base positions were covered with gray sheets in order to reduce visual inhomogeneity over the 314 m circumference circuit (figures 2 and 3). We were able to vary the density of cars in small steps of $10^{-2}\,\mathrm{m}^{-1}$.

Table 1. List of session ID and the number of cars. The last two digits of the session IDs express the number of cars N. The periods used in these analyses are set by discarding the beginning and the end of each session.

Start time	N (# of cars)	Total Running time (s)	Period used in analyses (s)	Session ID
8 December 2009				
13:12	10	431	150–400	1010
13:25	10	370	N/A	1110
13:33	10	380	0–250	1210
13:42	10	413	50–300	1310
13:56	12	465	100–350	1412
14:23	20	743	100–600	1520
14:42	25	892	350–750	1625
15:09	30	995	200–800	1730
15:47	35	1280	200–1000	1835
16:21	40	979	300–900	1940
9 December 2009				
10:58	30	817	100–700	2030
11:16	25	622	100–500	2125
11:34	28	636	100–450	2228
13:03	28	498	100–350	2328
13:18	32	824	100–700	2432
13:40	34	769	100–600	2534
14:15	34	902	150–700	2634
14:35	32	747	150–700	2732
14:58	30	743	100–600	2830
15:24	34	421	100–300	2934

In the previous experiment [9, 10] we read car positions manually from video data captured by a 360° camera; the positional error in this case was roughly ±0.5 m. In this experiment, we employed a laser scanner (Sick LD-LRS 1000) located at the center of the circuit (figure 3) to measure car positions with an improved resolution. The scanner rotated at a frequency of 5 Hz, detecting the distance to objects every 1/1920°; the resulting time resolution was 10^{-4} s, while the spatial resolution was 0.16 m at a distance of 50 m. The stream of data was stored in a computer connected to the scanner, allowing sequences of position and speed for each car to be reconstructed using the procedure shown in appendix A.

Over 2 days we conducted 19 sessions, with the number of cars for each session varying from 10 to 40. All of the cars were of the same model and specifications (Toyota Vitz: 1.3 L, 3885 mm long, automatic transmission). The conditions for each session are summarized in table 1 (1010, 1210, 1310 and 1412 were warm-up sessions).

Fifty-two college students drove the cars by turns. In each session the cars entered the circuit one by one, with the driver of the first car requested to drive slowly until all the cars had entered, at which point all of the drivers were instructed to drive safely in their own manner at a target speed of 30 km h^{-1}.

IOP Institute of Physics ⓘ DEUTSCHE PHYSIKALISCHE GESELLSCHAFT

3. Analyses

In order to locate dynamical phase transitions between free and jammed flows, we analyzed the data using spacetime diagrams, fluctuations in speed and fundamental diagrams. We first look at spacetime diagrams showing the trajectories of all cars running in each session. Three typical examples of sessions with 25, 30 and 34 cars (sessions 2125, 2030 and 2534, respectively) are shown in figure 4. In session 2125 (25 cars), all cars run smoothly, as shown in figure 4(a); density fluctuation occurs but does not lead to a traffic jam. Figure 4(b) shows the presence of a traffic jam in session 2030 (30 cars) in which cars undergo stop-and-go motion. A cluster of stopped or nearly stopped cars appears as stripes (sparse areas); this cluster moves backward at about $20 \, \text{km} \, \text{h}^{-1}$, which is about the same as cluster speeds observed on real expressways [9, 11]. In figure 4(c) representing session 2534 (34 cars), jam clusters in which cars move slowly appear and disappear. Spacetime diagrams for all sessions are shown in appendices B and C; these show that jammed flow occurs in high density conditions while free flow is maintained at low density.

The average speeds and fluctuations in speed are then analyzed in order to estimate the critical density for jam emergence. As can be seen in the observations and as discussed in section 1, the average speed of a jammed flow decreases as car density increases. Because cars run slow in jam clusters and fast outside of them, fluctuations in speed become large when there is jammed flow, and therefore the presence of large speed fluctuations indicates jammed flow.

For each session, the average speed and the fluctuation (defined as the standard deviation) are calculated for all cars over the period shown in table 1, with the results shown in figure 5. On both days, the average speed decreases as the car density increases. In sessions conducted on the first day, fluctuation does not increase with the density; on the second day, however, fluctuation increases with density, as is observed on a real expressway. This disparity seems to have arisen from the fact that the drivers were extremely cautious on the first day and did not appear to drive at the desired speed; correspondingly, we used data only from the warm-up sessions and from the second day for the remainder of the analysis. Large fluctuations around the average speed can be observed for sessions having between 28 and 34 cars on the second day, indicating that traffic jams occurred in these sessions.

Finally, we examined the fundamental diagrams representing the density–flow relation. On real expressways, speed and flow are measured using induction-loop coils buried beneath observational points on a road, with the average speed v and flow q recorded, for example, every 5 min. The density ρ at a given point in time then is calculated from the relation $q = \rho v$. Three typical observational features of a fundamental diagram for a real expressway (e.g. figure 1) are [11–13]: free flow is shown as data points on a single curve; in jammed flow, the data points are broadly scattered; and both free and jammed flows occur at intermediate densities.

In order to determine an appropriate method of averaging the data for obtaining a fundamental diagram for the experiment, we set three observational points spaced at intervals of $120°$ for collecting a sufficient number of data points. At each observational point, we count the number of cars passing by over intervals of 45 s, a duration based on the time needed for a jam cluster to move around the circuit and averaged their speeds.

As a comparison, appendix D shows fundamental diagrams with a duration of 30 s; these exhibit essentially the same characteristics as are discussed below. For reference, the fundamental diagram of the sessions (including the warm-up) on the first day is shown in appendix E.
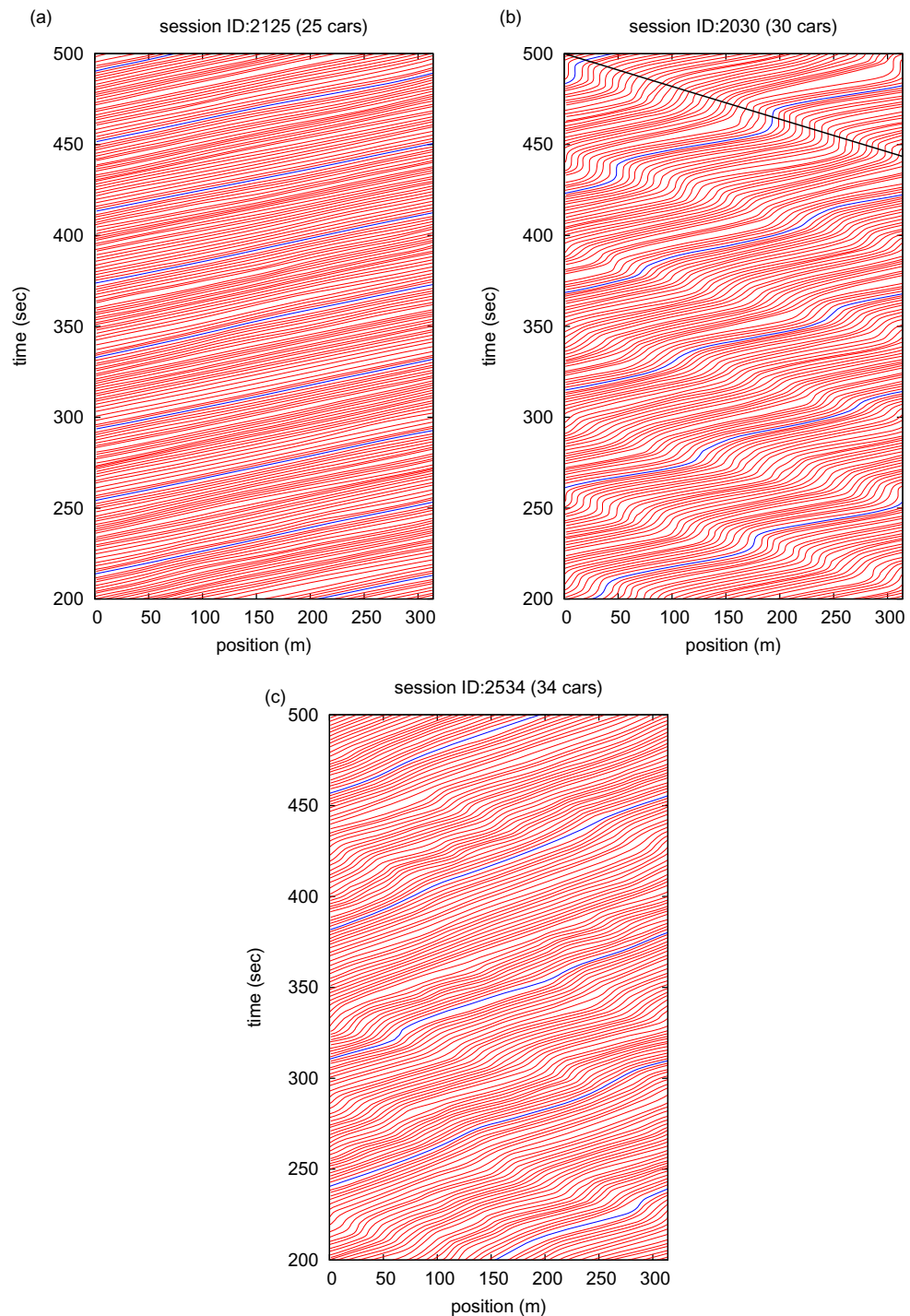
Figure 4. Spacetime diagrams for three sessions (2125, 2030 and 2534) with 25, 30 and 34 cars. The vertical axis is time (s) and the horizontal axis is position (m). The blue curves correspond to the trajectory of each of the cars. In session 2125 (a), all cars run smoothly. In session 2030 (b), a cluster of stopped or almost-stopped cars (stripes of sparse curves) propagates backward with a speed of about $20 \, \mathrm{km \, h^{-1}}$, as represented by the black line. In session 2534 (c), jam clusters appear and disappear.
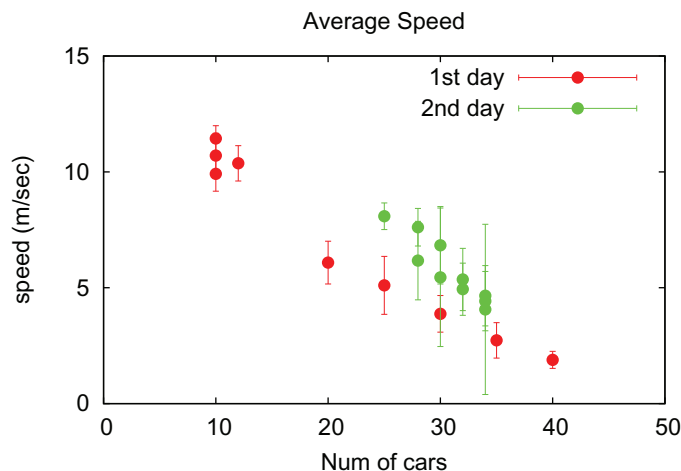
Figure 5. Average speed by number of cars. The vertical bars show the standard deviation for each session; the red and green marks show data for sessions on the first and the second days, respectively.
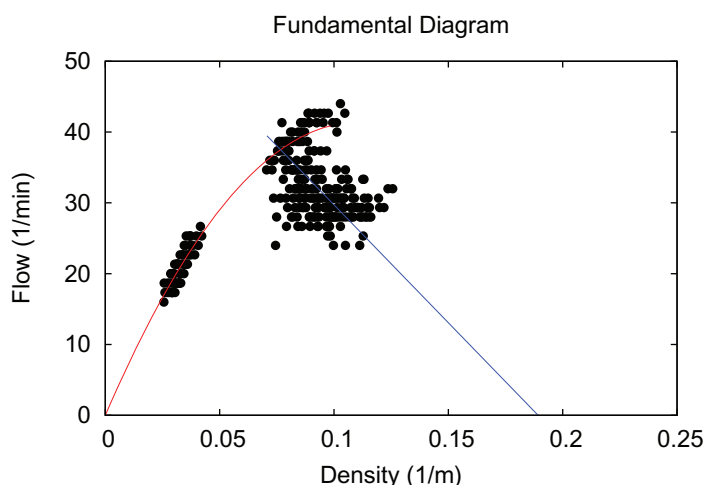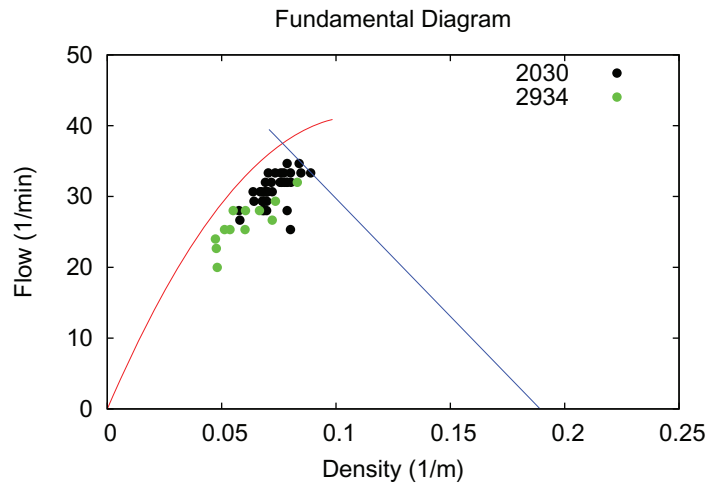

Figure 6. Fundamental diagram for the selected sessions excluding 2030 and 2934. The red curve and the blue line are drawn as references to show the typical behavior of free and jammed flows.

Figure 6 shows the fundamental diagram for all sessions except for 2030 and 2934, which are excluded for reasons discussed at the end of this section. This fundamental diagram is similar to that extracted from traffic on real expressways (figure 1), and on it we find three typical features: free flow, jammed flow and metastable states. The red curve and the blue line in figure 6 are drawn as references to show the typical behavior of free and jammed flows, respectively.

In the following paragraphs, we investigate the characteristic features of the fundamental diagram in detail. Figure 7(a) shows the fundamental diagram for the sessions with small numbers of cars, $10 \leqslant N \leqslant 25$. Here, the flow is an increasing function of the density, which is a typical feature of free flow. The curve in figure 7(a) is drawn for reference by fitting the data
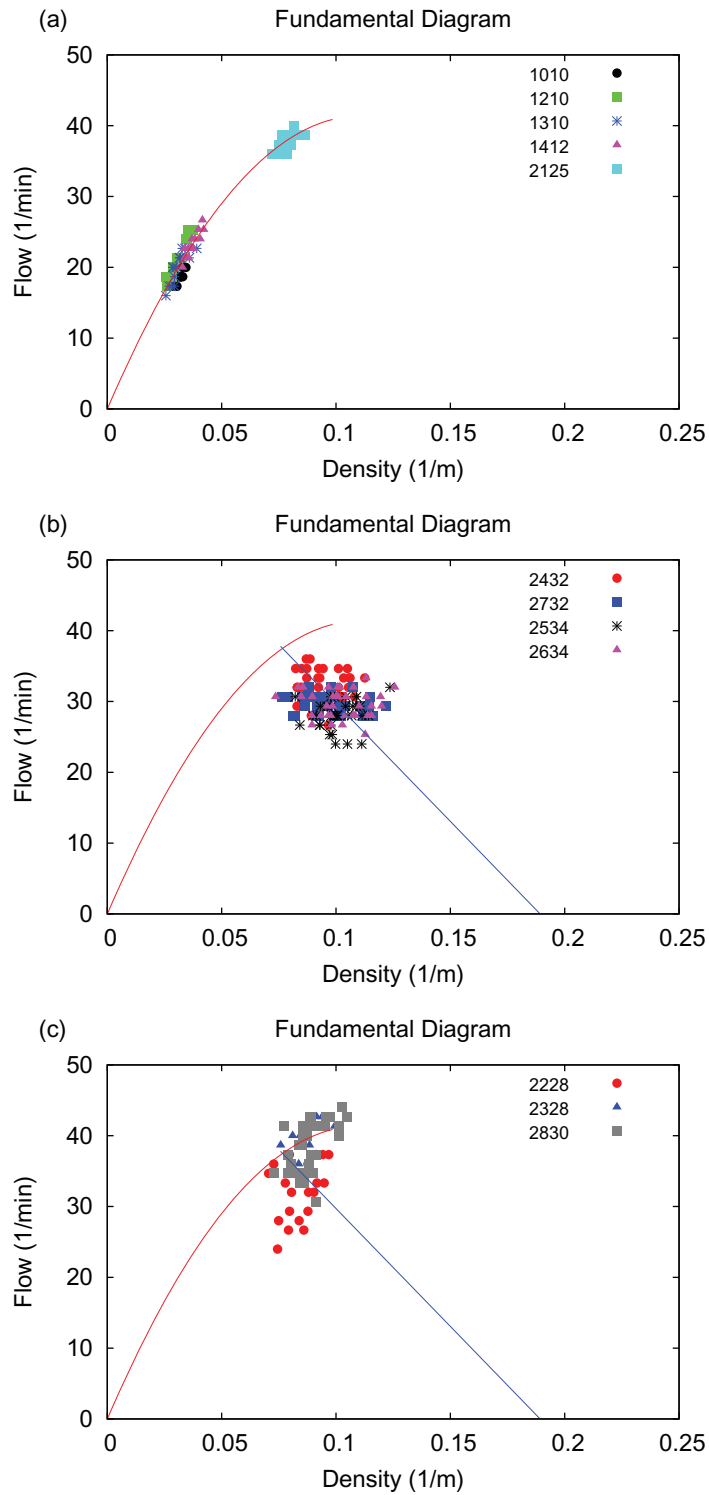
Figure 7. Fundamental diagrams for (a) free flow, (b) jammed flow and (c) intermediate states. The red curve and the blue line are drawn as references for the typical behavior of free and jammed flows, respectively.

Figure 8. The fundamental diagram for sessions 2030 and 2934, in which jam clusters contain stopped or nearly stopped cars. The red curve and the blue line are drawn as references for the typical behavior of free and jammed flows, respectively.

points with a quadratic curve $a\rho - b\rho^2$, where a and b are the fitting parameters; a corresponds to the average speed in free flow and is estimated to be $a \sim 40\,\mathrm{km\,h^{-1}}$.

In figure 7(b), showing the fundamental diagram for sessions with large numbers of cars, from $N = 32\text{–}34$, the data points are broadly scattered, a feature that indicates the inhomogeneity of the flow; in other words, traffic jams occur in these sessions. The line $-c(\rho - d)$ is obtained by fitting the data using $c = 20\,\mathrm{km\,h^{-1}}$ as the speed of the jam cluster (see figure 4) and d as a fitting parameter.

Figure 7(c) shows the fundamental diagram for sessions with intermediate numbers of cars, i.e. between $N = 28$ and 30. The portion of data points distributed broadly around the blue line correspond to jammed flow, while the remaining points that are distributed along the red line correspond to free flow. Thus, the sessions with intermediate numbers of cars have both free and jammed flows at a given density value; this indicates the presence of metastable states, which have previously been suggested by models and reported from observation [10, 12, 14–18].

The fundamental diagram for the two exceptional sessions 2030 and 2934, in which cars stop or nearly stop in jam clusters, is shown in figure 8. Because cars are only detected in passing by the observation point, stopped cars are not taken into account in the flow measurement or in the average speed and the fundamental diagram consists mainly of data from cars moving smoothly outside of jam clusters. Because the speeds of cars outside the jam cluster are nearly identical to those in free flow (see figures 4(a) and (b)), the diagram resembles that for a free flow, although it can be seen that the average speed is a bit smaller and the level of fluctuation is larger than in a 'true' free flow (figure 7(a)) because the motions of cars catching up with and escaping from the jam clusters are also included in the data.

Based on an analysis of the data in this section, we can estimate the value of the critical density of the dynamical phase transition between free and jammed flows. If the number of cars is $N \leqslant 25$, the fluctuation in speed is small (see figure 5) and the flow increases with density (see figure 7(a)); in such cases, free flow occurs.

If on the other hand the number of cars is $N \geqslant 28$, jammed flows occur where fluctuations in speed are large (see figure 5), and the data in the fundamental diagram are broadly scattered (see figures 7(b) and (c)). Thus, we can conclude that critical density occurs between $0.08\,\mathrm{m}^{-1}$ ($N = 25$) and $0.09\,\mathrm{m}^{-1}$ ($N = 28$).

4. Summary and discussions

We conducted the experiment described in this paper to confirm that the emergence of a traffic jam is a dynamical phase transition controlled by the density of cars. In our previous study [9, 10], which was conducted on an outdoor field, we demonstrated that a traffic jams occurs at a certain high density even in the absence of bottlenecks. The present study consisted of 19 sessions in which the number of cars was varied from 10 to 40. The experiment was carried out on an indoor circuit 314 m in circumference with high resolution measurements (i.e. 0.2 s in time and 0.16 m in space). Based on our analysis of the resulting spacetime diagrams, fluctuations in speed and fundamental diagrams, we confirmed that dynamical phase transition between free and jammed flow occurs at a critical density, which we were able to estimate. We also observed that metastable states occur at intermediate densities between free and jammed flows.

We can compare the critical density obtained in this study with those measured on real expressways. The critical density of an expressway in which the observed average speed is $120\,\mathrm{km\,h}^{-1}$ in free flow is known to be $\rho \sim 0.025\,\mathrm{m}^{-1}$ ($25\,\mathrm{cars\,km}^{-1}$) [9]. In our present experiment in which the average speed in free flow was about $40\,\mathrm{km\,h}^{-1}$ (figure 7(a)), critical density occurred between 0.08 and $0.09\,\mathrm{m}^{-1}$. As a car will require a headway that is three times larger when driving three times faster, our measured experimental critical density is consistent with values observed on the expressway.

We then assess our fundamental diagram for jammed flow with stopped cars. A look at figure 8 will confirm that the fundamental diagram for such a flow is different from that for a jammed flow without stopped cars (figure 7(b)); instead, it resembles the fundamental diagram for free flow. Fundamental diagrams for stop-and-go traffic with this kind of similarity to free flow diagrams have been generated from real expressway data [19]. However, the spacetime diagrams for stop-and-go traffic are essentially identical to those for jammed flow without stopped cars. As a fundamental diagram describes the relation between the number of cars passing by a measurement point and the density, the fundamental diagram of jammed flow will always differ depending on whether or not it contains stopped cars; however, this does not mean that stop-and-go traffic represents a different phase from jammed flow without stopped cars.

In this paper, we discussed the phase transition based on conventional observables, such as fundamental diagrams, measured in real expressways and we did not mention any models, because we hoped to estimate the critical density without depending on any models by comparing observed phenomena in real expressways. We showed that the transition between free and jammed flow occurs at a critical density and metastable states appear around the critical density. In this sense, the transition seems to be first order. However, it is different from phase transitions of ordinary equilibrium systems. As for a traffic flow, particles (cars) in the system are moving, and emerged patterns (jam clusters) also move. The phenomenon should be identified as dynamical transition.

The order parameter for describing the transition is not confirmed yet, but the change of the correlations in motions of cars is characteristic. In a free flow, speed of cars fluctuate randomly

and there are almost no long-range correlations. In a jammed flow, by contrast, jam clusters induce correlations in motions of cars. Therefore correlations in motions of cars will indicate the occurrence of traffic jam. By analyzing trajectories of cars obtained in this experiment, we hope to discuss about correlations, order-parameters describing the phase transition, model selections and so on.

Finally, we can analyze a case with extremely high density. Figure 5 shows that the fluctuation in speed is very small in the session with 40 cars; as shown in the spacetime diagram, the flow is homogeneous (figure C.2 in appendix C). Some theoretical models predict that homogeneous flow exceeding a certain high density will also be stable [17, 20]; however, it is not clear at present that the observed high density–flow in this case corresponds to that predicted by models.

Acknowledgments

Appendix A. Data acquisition

A rotating scanner ejects laser pulses and measures distance by detecting the reflected pulses from an object. The distance to the object is recorded accompanied with a time stamp and the angle of rotation of the scanner. In this way, the distance to a car or to the surrounding wall of the arena can be measured. When a pulse is reflected by a car, the measured distance should be around 50 m. We can identify about 24 ($\simeq 3.9/0.16 =$ (car length)/(space resolution)) successive data points at such distance as equivalent to a single car at the present resolution. Errors owing to lack of reflection are corrected heuristically.

Because of the rotation of the laser scanner, the heads and tails of the successive data series for a single car are recorded with different time stamps; correspondingly, we use the midpoint between the head and the tail to determine the time t_i of observation and the position $x^{\mathrm{r}}(t_i)$ of the car, where i denotes the sequential index of the time of observation for the car.

The positions of the cars are recorded about every 0.2 s, and for each car a sequence of raw data such as $\{x^{\mathrm{r}}(t_i)\}$ is obtained. These data still contain jagged noises, which prevents the direct calculation of car speeds; therefore, a smoothed value of the position $x^{\mathrm{s}}(t_i)$ is calculated as an average of three successive raw data points as follows:

$$x^{\mathrm{s}}(t_i) = \tfrac{1}{4}\left(x^{\mathrm{r}}(t_{i-1}) + 2x^{\mathrm{r}}(t_i) + x^{\mathrm{r}}(t_{i+1})\right). \tag{A.1}$$

The speed v^{s} of a car at $(t_i + t_{i+1})/2$ is then obtained using the smoothed car positions as:

$$v^{\mathrm{s}}\left(t_i'\right) = \frac{x^{\mathrm{s}}(t_{i+1}) - x^{\mathrm{s}}(t_i)}{t_{i+1} - t_i}, \quad t_i' = \frac{t_i + t_{i+1}}{2}. \tag{A.2}$$

Values of position and speed on equal-time slices of every 0.2 s are obtained using linear interpolation and are analyzed over a period set so that data points from the beginning and end of each session the discarded.
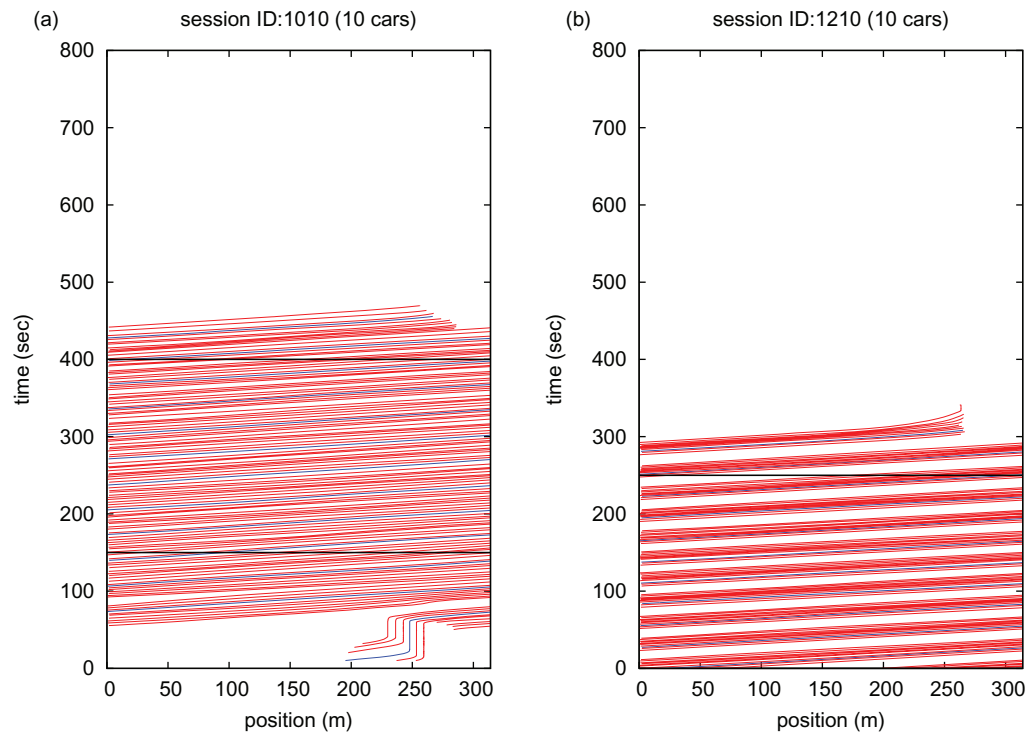
Figure B.1. Spacetime diagram for sessions 1010 and 1210. The vertical axis shows time (s) and the horizontal axis shows position (m). Each blue curve represents the trajectory of one car. Black horizontal lines indicate the periods used for analysis.

Appendix B. Spacetime diagrams of sessions used in analyses

In the main text we analyzed data taken from four of the warm-up sessions on the first day and all sessions on the second day. This appendix shows the spacetime diagrams for these sessions in figures B.1–B.4. The periods used for analyses in the main text are indicated by black horizontal lines.

Appendix C. Spacetime diagrams of sessions unused in analyses

We performed nine sessions during the first day. Data obtained in four warm-up sessions were used in the analysis; spacetime diagrams for the five remaining sessions are shown in figures C.1 and C.2. The periods used for analysis in the main text and appendix E are indicated by black horizontal lines.

Appendix D. Fundamental diagrams using shorter duration

In the main text we counted the number of cars passing by a measuring point over intervals of 45 s and averaged the speeds measured at each observational point. For comparison, we show here fundamental diagrams based on a 30 s observational duration. Figure D.1 shows the
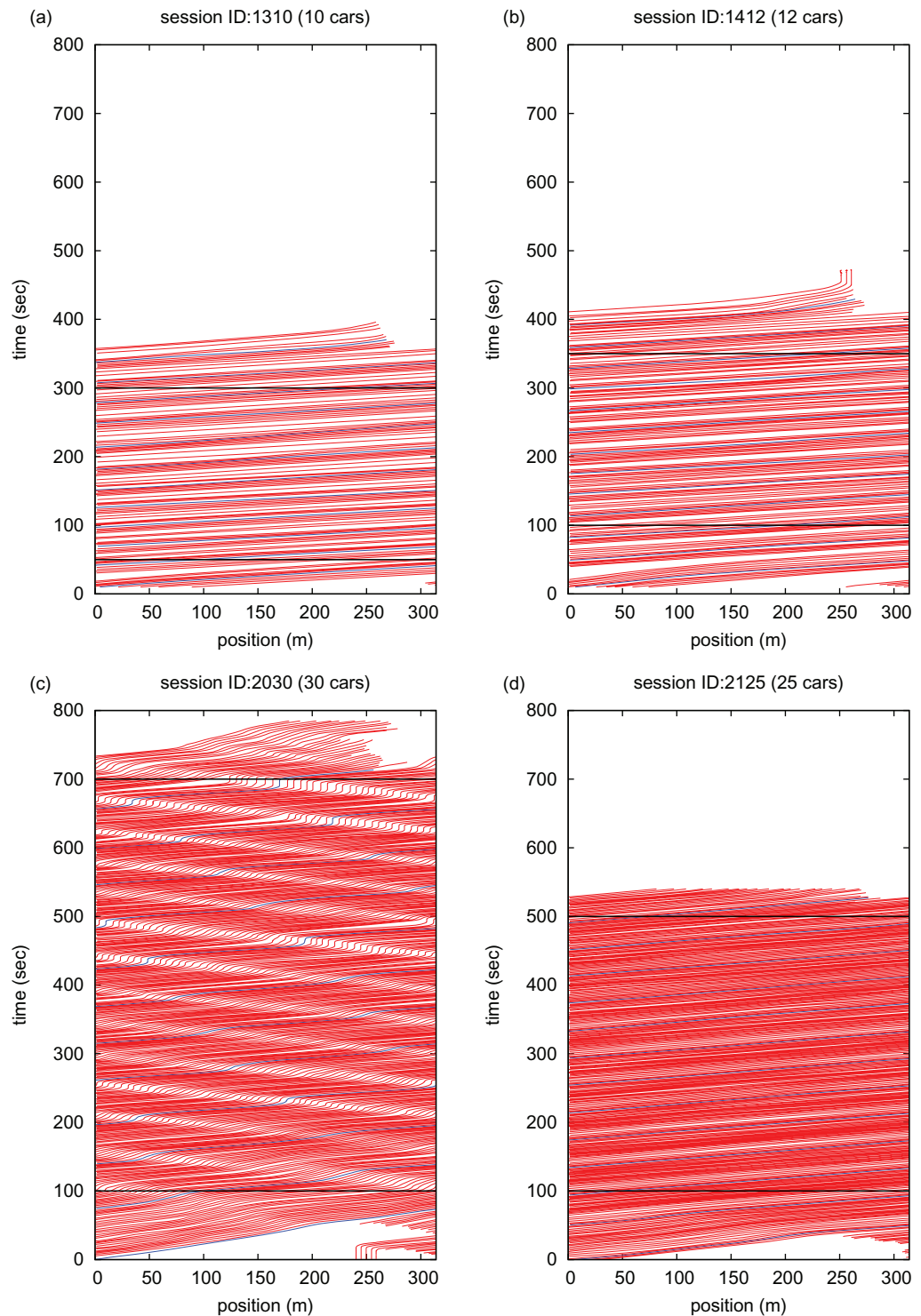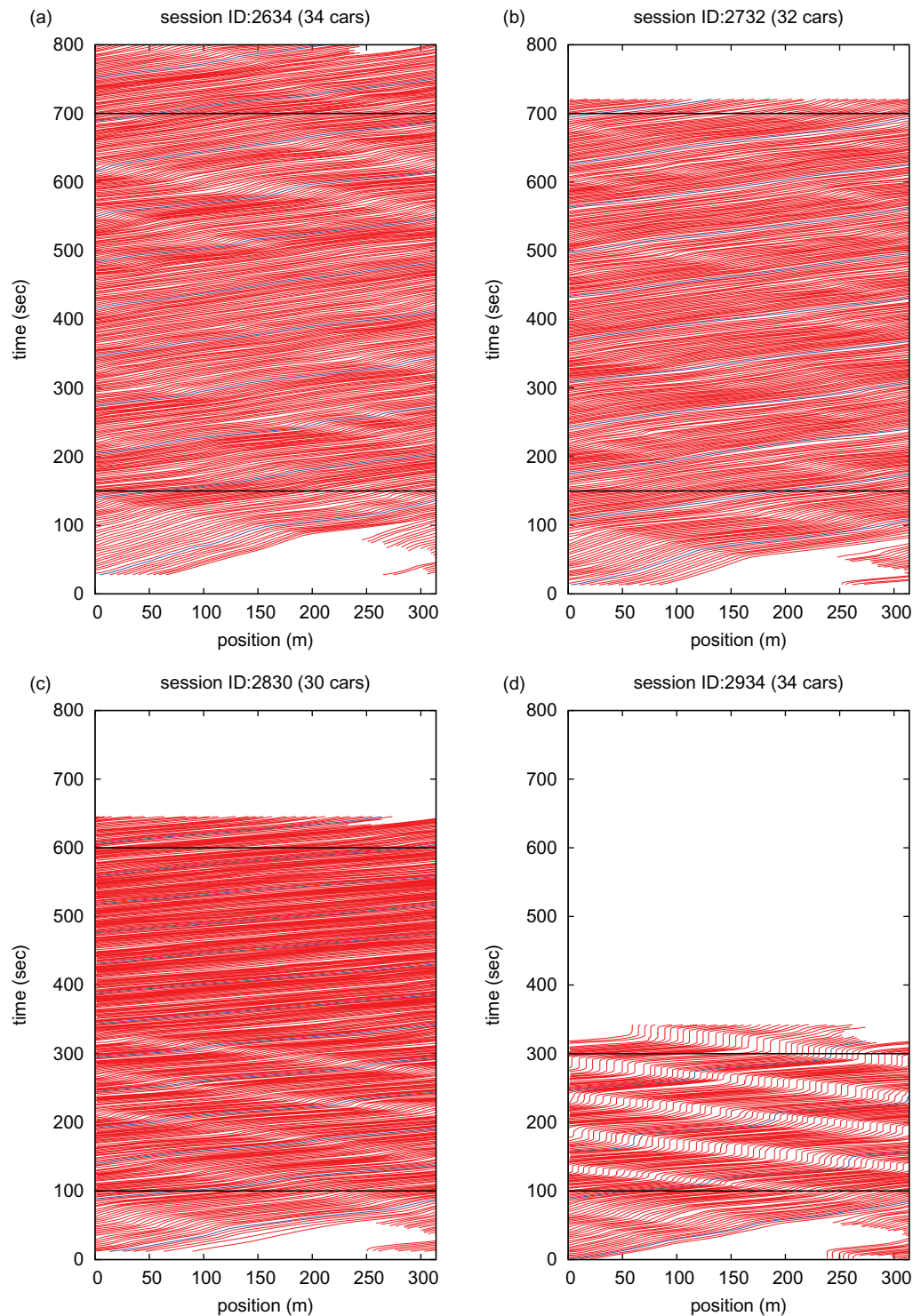
Figure B.2. Spacetime diagram for sessions 1310, 1412, 2030 and 2125. The vertical axis shows time (s) and the horizontal axis shows position (m). Each blue curve represents the trajectory of one car. Black horizontal lines indicate the periods used for analysis.
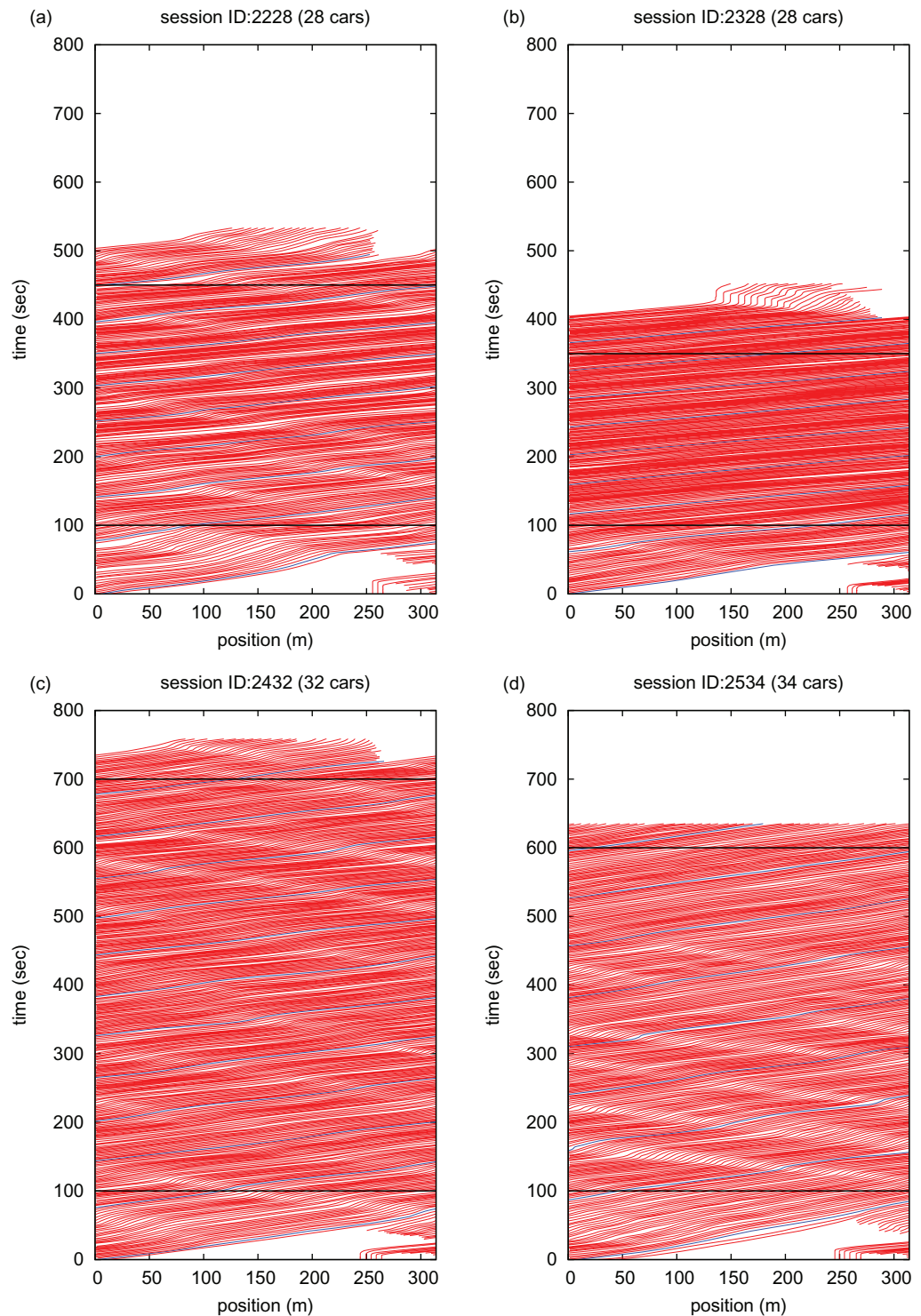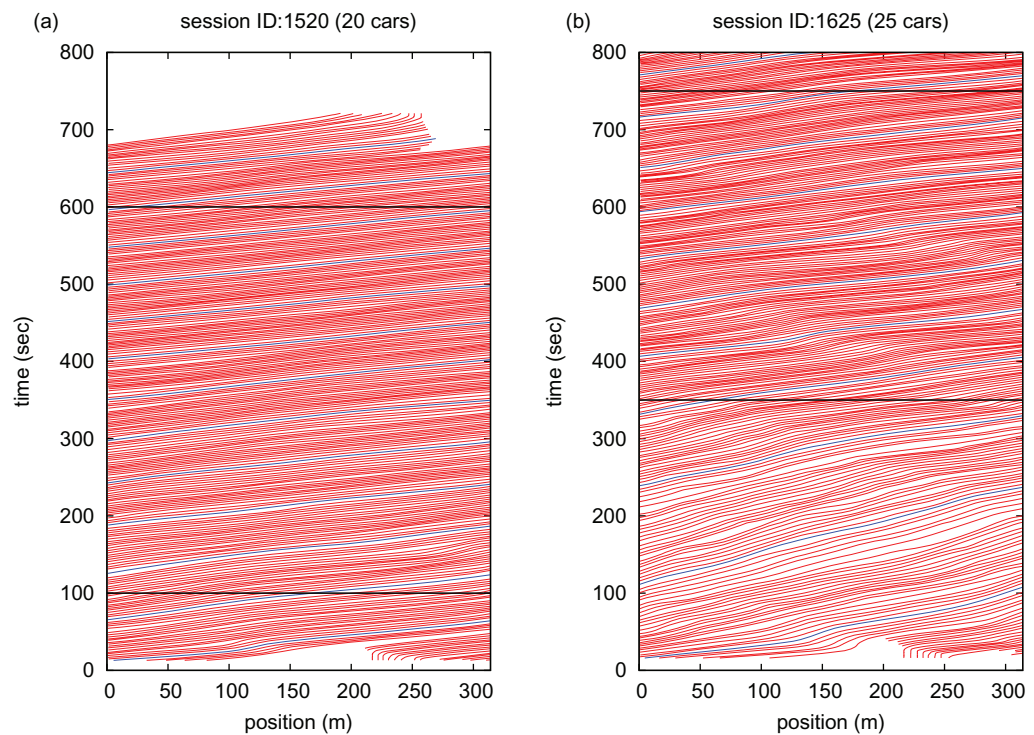
Figure B.3. Spacetime diagram for sessions 2228, 2328, 2432 and 2534. The vertical axis shows time (s) and the horizontal axis shows position (m). Each blue curve represents the trajectory of one car. Black horizontal lines indicate the periods used for analysis.

Figure B.4. Spacetime diagram for sessions 2634, 2832, 2830 and 2934. The vertical axis shows time (s) and the horizontal axis shows position (m). Each blue curve represents the trajectory of one car. Black horizontal lines indicate the periods used for analysis.
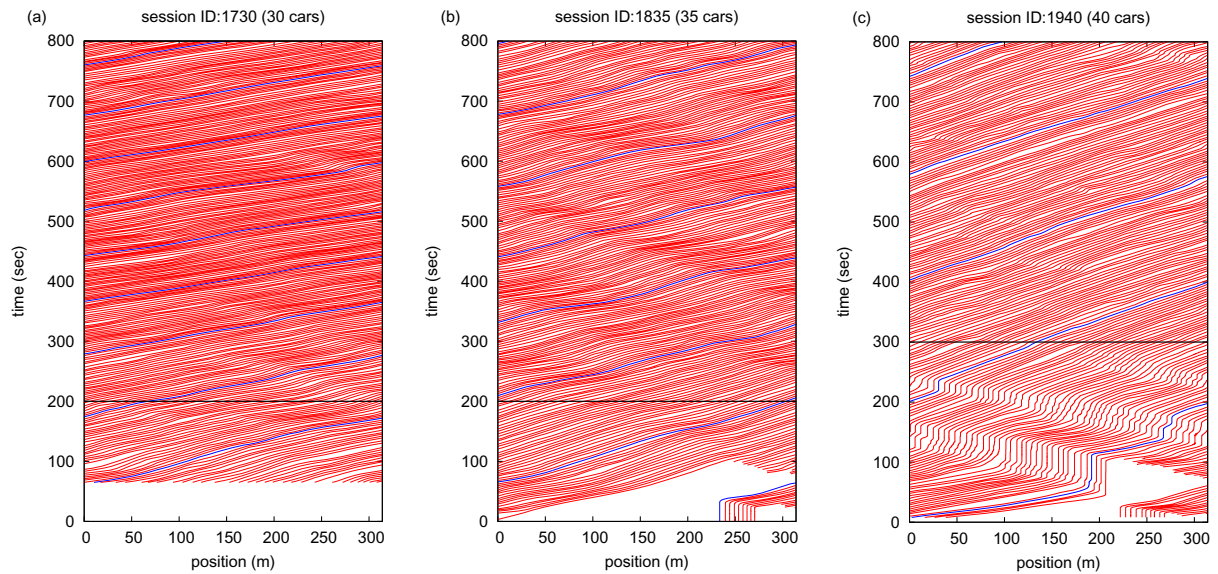
Figure C.1. Spacetime diagram for sessions 1520 and 1526. The vertical axis shows time (s) and the horizontal axis shows position (m). Each blue curve represents the trajectory of one car. Black horizontal lines indicate the periods used for analysis.

fundamental diagram for selected sessions with the exception of 2030 and 2934. Though the data are scattered more broadly than those in figure 6 with 45 s duration, we can see the similar characteristics in figure 6.

As discussed in section 4, the fundamental diagrams for jammed flow containing stopped cars appear to be similar to those with free flow. Figure D.2 shows the fundamental diagram for 30 s measurement duration for sessions 2030 and 2934, in which the jam clusters contain stopped cars. Compared with figure 8, the occurrences of stop-and-go traffic are less similar to those with free flow.

Appendix E. Fundamental diagram for sessions on the first day

In the main text we analyzed data obtained from warm-up sessions and from sessions conducted on the second day. Here, we show the fundamental diagram for sessions conducted on the first day including the warm-up sessions, in figure E.1. The duration of observation is 45 s, as described in the main text.

Figure C.2. Spacetime diagram for the sessions 1730, 1835 and 1940. The vertical axis shows time (s) and the horizontal axis shows position (m). Each blue curve represents the trajectory of one car. Black horizontal lines indicate the periods used for analysis.
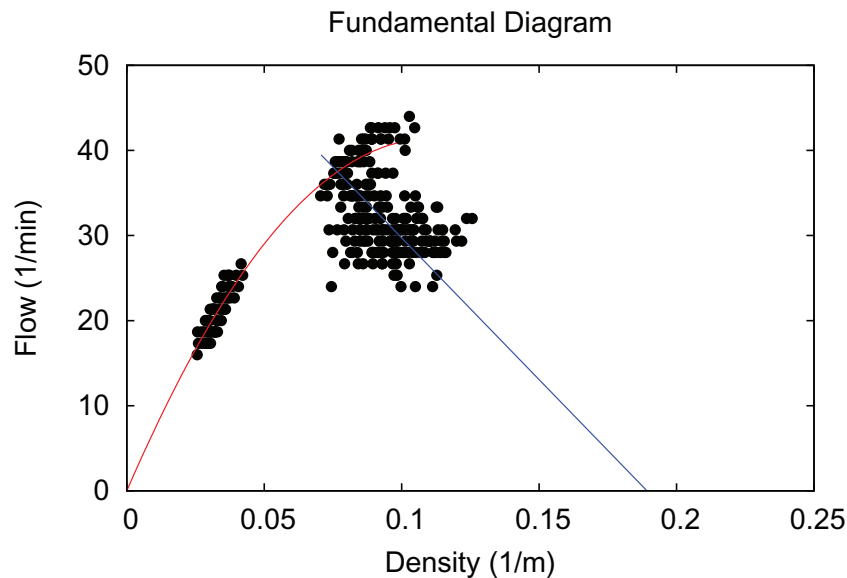

Figure D.1. The fundamental diagram for all selected sessions except 2030 and 2934.

The red curve and the blue line are the same as those in figure 6. The data points for all sessions except for the warm-up sessions are distributed below the blue line, demonstrating that cars on the first day, except those in the warm-up sessions, ran more slowly than those in sessions with the same number of cars on the second day.

IOP Institute of Physics Φ DEUTSCHE PHYSIKALISCHE GESELLSCHAFT

Fundamental Diagram
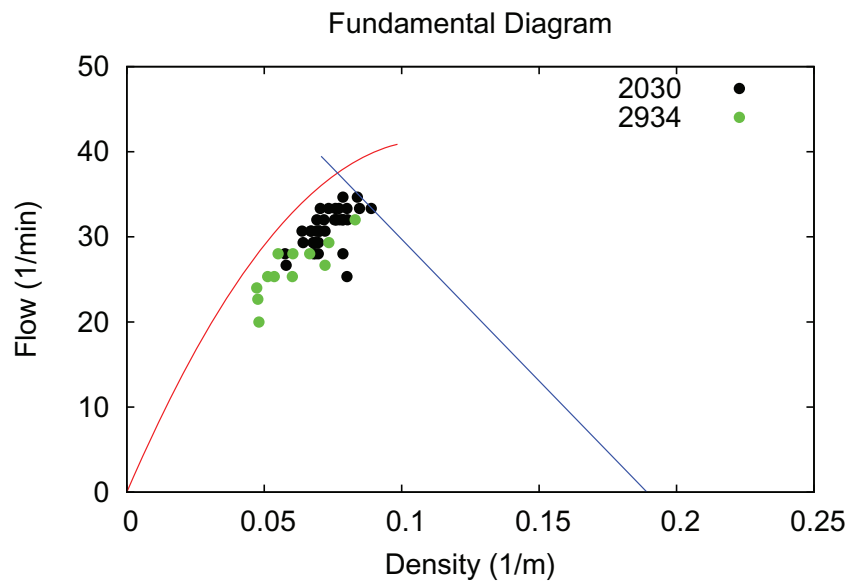
Figure D.2. The fundamental diagram for sessions 2030 and 2934, in which jam clusters contain stopped cars.

Fundamental Diagram
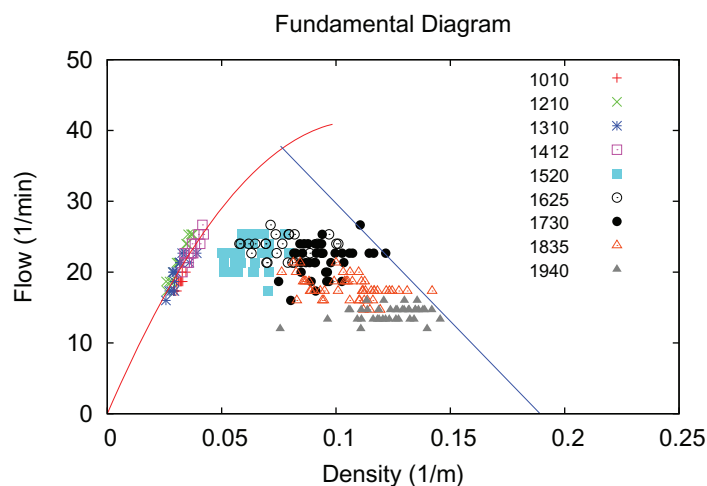
Figure E.1. Fundamental diagram for sessions on the first day. The red curve and blue line are drawn as references for typical behavior of free and jammed flows, respectively.

References

[1] Leutzbach W 1972 *Introduction to the Theory of Traffic Flow* (Berlin: Springer)
[2] Wolf D E, Schreckenberg M and Bachem A (ed) 1996 *Workshop on Traffic and Granular Flow* (Singapore: World Scientific)
[3] Chowdhury D, Santen L and Schadschneider A 2000 Statistical physics of vehicular traffic and some related systems *Phys. Rep.* **329** 199–329
[4] Helbing D 2001 Traffic and related self-driven many-particle systems *Rev. Mod. Phys.* **73** 1067–141
[5] Nagatani T 2002 The physics of traffic jams *Rep. Prog. Phys.* **65** 1331

[6] Fukui M, Sugiyama Y, Schreckenberg M and Wolf D E (ed) 2003 *Traffic and Granular Flow '01* (Berlin: Springer)

[7] Kerner B S 2004 *The Physics of Traffic* (Berlin: Springer)

[8] Kerner B S 2009 *Introduction to Modern Traffic Flow Theory and Control: The Long Road to Three-Phase Traffic Theory* (Berlin: Splinger)

[9] Sugiyama Y, Fukui M, Kikuchi M, Hasebe K, Nakayama A, Nishinari K, Tadaki S and Yukawa S 2008 Traffic jams without bottlenecks—experimental evidence for the physical mechanism of the formation of a jam *New. J. Phys.* **10** 033001

[10] Nakayama A, Fukui M, Kikuchi M, Hasebe K, Nishinari K, Sugiyama Y, Tadaki S and Yukawa S 2009 Metastability in the formation of an experimental traffic jam *New. J. Phys.* **11** 083025

[11] Yukawa S, Kikuchi M, Nakayama A, Nishinari K, Sugiyama S and Tadaki S 2003 Observational aspects of Japanese highway traffic *Traffic and Granular Flow '01* ed M Fukui, Y Sugiyama, M Schreckenberg and D E Wolf (Berlin: Springer) pp 243–56

[12] Kikuchi M, Nakayama A, Nishinari K, Sugiyama S, Tadaki S and Yukawa S 2003 Long-term traffic data from Japanese expressway *Traffic and Granular Flow '01* ed M Fukui, Y Sugiyama, M Schreckenberg and D E Wolf (Berlin: Springer) pp 257–62

[13] Tadaki S, Nishinari K, Kikuchi M, Sugiyama Y and Yukawa S 2002 Analysis of congested flow at the upper stream of a tunnel *Physica* A **315** 156–62

[14] Kerner B S 1998 Experimental features of self-organization in traffic flow *Phys. Rev. Lett.* **81** 3797–800

[15] Barlovic R, Santen L, Schadschneider A and Schreckenberg M 1998 Metastable states in cellular automata for traffic flow *Eur. Phys. J.* B **5** 793–800

[16] Nishinari K, Fukui M and Schadschneider A A 2004 stochastic cellular automaton model for traffic flow with multiple metastable states *J. Phys. A: Math. Gen.* **37** 3101–10

[17] Bando M, Hasebe K, Nakanishi K, Nakayama A, Shibata A and Sugiyama Y 1995 Phenomenological study of dynamical model of traffic flow *J. Phys. I France* **5** 1389–99

[18] Kanai M, Nishinari K and Tokihiro T 2005 Stochastic optimal velocity model and its long-lived metastability *Phys. Rev.* E **72** 035102

[19] Neubert L, Santen L, Schadschneider A and Schreckenberg M 1999 Single-vehicle data of highway traffic: a statistical analysis *Phys. Rev.* E **60** 6480–90

[20] Bando M, Hasebe K, Nakayama A, Shibata A and Sugiyama Y 1995 Dynamical model of traffic congestion and numerical simulation *Phys. Rev.* E **51** 1035–42